Journal of Controlled Release 343 (2022) 207–216

Contents lists available at ScienceDirect

Journal of Controlled Release

journal homepage: www.elsevier.com/locate/jconrel

Delivery of modified mRNA to damaged myocardium by systemic administration of lipid nanoparticles

Martijn J.W. Evers [a,1], Wenjuan Du [b,f,1], Qiangbing Yang [a], Sander A.A. Kooijmans [a], Aryan Vink [d], Mies van Steenbergen [g], Pieter Vader [a,b], Saskia C.A. de Jager [b], Sabine A. Fuchs [e], Enrico Mastrobattista [g], Joost P.G. Sluijter [b,c], Zhiyong Lei [a,b], Raymond Schiffelers [a,*]

[a] CDL Research, UMC Utrecht, Utrecht, the Netherlands
[b] Department of Experimental Cardiology, Circulatory Health Laboratory, UMC Utrecht, Utrecht, the Netherlands
[c] Regenerative medicine Centre, UMC Utrecht, University Utrecht, Utrecht, the Netherlands
[d] Department of Pathology, UMC Utrecht, Utrecht, the Netherlands
[e] Division of Pediatric Gastroenterology, Wilhelmina Children's Hospital, UMC Utrecht, Utrecht, the Netherlands
[f] Department of Cardiology, The Second Affiliated Hospital of Harbin Medical University, Harbin, Heilongjiang Province, PR China
[g] Department of Pharmaceutics, Utrecht Institute for Pharmaceutical Sciences (UIPS), Faculty of Science, Utrecht University, P.O. Box 80082, 3508 TB Utrecht, the Netherlands.

ARTICLE INFO

Keywords:
Modified mRNA
Lipid nanoparticles
Myocardial infarction
Systemic delivery
Reperfusion injury

ABSTRACT

Lipid Nanoparticles (LNPs) are a promising drug delivery vehicle for clinical siRNA delivery. Modified mRNA (modRNA) has recently gained great attention as a therapeutic molecule in cardiac regeneration. However, for mRNA to be functional, it must first reach the diseased myocardium, enter the target cell, escape from the endosomal compartment into the cytosol and be translated into a functional protein. However, it is unknown if LNPs can effectively deliver mRNA, which is much larger than siRNA, to the ischemic myocardium. Here, we evaluated the ability of LNPs to deliver mRNA to the myocardium upon ischemia-reperfusion injury functionally. By exploring the bio-distribution of fluorescently labeled LNPs, we observed that, upon reperfusion, LNPs accumulated in the infarct area of the heart. Subsequently, the functional delivery of modRNA was evaluated by the administration of firefly luciferase encoding modRNA. Concomitantly, a significant increase in firefly luciferase expression was observed in the heart upon myocardial reperfusion when compared to sham-operated animals. To characterize the targeted cells within the myocardium, we injected LNPs loaded with Cre modRNA into Cre-reporter mice. Upon LNP infusion, Tdtomato+ cells, derived from Cre mediated recombination, were observed in the infarct region as well as the epicardial layer upon LNP infusion. Within the infarct area, most targeted cells were cardiac fibroblasts but also some cardiomyocytes and macrophages were found. Although the expression levels were low compared to LNP-modRNA delivery into the liver, our data show the ability of LNPs to functionally deliver modRNA therapeutics to the damaged myocardium, which holds great promise for modRNA-based cardiac therapies.

1. Introduction

Despite the advances in healthcare, heart failure is still one of the leading causes of death worldwide [1]. One of the most prevalent causes of heart failure is myocardial infarction. Part of the myocardium is starved of blood supply due to the occlusion of a coronary artery resulting in the loss of billions of cardiomyocytes [2]. Due to the limited regenerative capacity of the heart [3] and the lack of appropriate therapeutic interventions [4], the damaged heart has to compensate for the loss of cardiomyocytes via compensatory outward remodeling of the myocardium. This leads to the expansion of the infarction area and eventually results in heart failure [1].

Stimulating cardiac repair and regeneration could be a potential therapeutic intervention to stop remodeling of the injured heart [4]. In the past years, researchers have identified several processes involved in cardiac development and regeneration [3]. Examples are the Hippo-Yap

* Corresponding authors.
E-mail addresses: j.sluijter@umcutrecht.nl (J.P.G. Sluijter), zlei@umcutrecht.nl (Z. Lei), R.Schiffelers@umcutrecht.nl (R. Schiffelers).
[1] These authors contributed equally to this work.

https://doi.org/10.1016/j.jconrel.2022.01.027
Received 11 September 2021; Received in revised form 15 January 2022; Accepted 18 January 2022
Available online 22 January 2022

pathway [5–7], growth factors like NRG1 [8,9], VEGFA [10] and FGF2 [11,12], and the ability to reprogram fibroblast into cardiomyocytes [13,14], which can be exploited to stimulate cardiac repair and regeneration in order to prevent pathological development of heart failure after myocardial infarction. However, these studies used transgenic animals [6–9,11], direct injection of recombinant protein [10–12] or a viral approach [5,13,14] to increase the expression of specific proteins. Though these methods are very useful for proof of concept studies, they have limited clinical translatability due to either the potential immunogenicity and carcinogenicity of viral vectors [15] or the extremely short half-life of the delivered therapeutic proteins [16].

Recent developments in the design and production of modified mRNA (modRNA) have significantly enhanced mRNA stability and reduced its immunogenicity [17–19]. These improvements helped modRNA emerge as an alternative to the genetic or viral approaches for the delivery of genetic material. The administration of naked VEGF [20] and FSTL1 [21] modRNA into the myocardium has shown promising effects on vascular regeneration, cardiomyocytes proliferation after myocardial infarction [20,21].

However, administration of naked modRNA delivery is challenging since modRNA's physicochemical properties, including their large size and negative charge, make the spontaneous crossing of the cellular membrane virtually impossible [19]. Besides, direct administration of naked modRNAs to the myocardium requires direct intramyocardial injection via catheter-based intramyocardial delivery or invasive open chest surgery. Moreover, these methods come with the inavoidable quick removal pitfall via venous drainage observed for cell injection [22]. Therefore, modRNA's therapeutic delivery would benefit from a drug delivery system that could provide sufficient protection to the modRNA therapeutics, allow systemic administration with significant enrichment in the targeted disease domain. Lipid nanoparticles (LNPs) are one such delivery system.

The occlusion of the coronary artery results in vascular endothelium leakage , which enables nanoparticles to extravasate from the circulation in the ischemic area [23]. In line with these findings, we have shown that a lipid-based nanoparticle can access the myocardium after myocardial infarction, probably due to damage-induced vascular permeability: a phenomenon that is not observed in the healthy myocardium [24]. However, it is unknown whether such an approach also allows the delivery of functional modRNA to the damaged myocardium. This study exploits the feasibility of using LNPs for functional delivery of modRNAs to the injured myocardium upon reperfusion.

2. Materials & methods

2.1. Synthesis of DLin-MC3-DMA

2.1.1. Synthesis of DLin-MeOH

DLin-MeOH was synthesized according to the protocol reported before, with minor adaptions [25]. In short: Mg Turnings(2.2 g, 100 mmol) were added to a dry 500 mL three-neck round-bottom (RB) flask equipped with a magnetic stirring bar, fluid cooled condenser and addition funnel. The setup was flushed with nitrogen and then 10 mL of anhydrous ether was added to the RB flask. Lineoleyl Bromide (24.04 g, 73 mmol) was dissolved in 45 mL anhydrous ether and loaded in the addition funnel. ~2 mL of this solution was added to the MG turnings and an exothermic reaction was observed. Iodine flakes (5 mg) were added to the reaction mixture to confirm formation of the Grignard reagent and the ether started refluxing. 43 mL of the Lineolyl bromide was subsequently added dropwise. After the addition of Lineolyl bromide, the reaction was kept under reflux at 35 degrees for 1 h and then cooled in an ice bath. Ethyl Formate (2.46 g, 33.18 mmol) was dissolved in 35 mL anhydrous ether, transferred to the addition funnel and then added to the reaction mixture. The reaction was stirred for 1 h at room temperature. The reaction was then quenched by dropwise addition of 4 mL acetone and 24 mL of ice-cold water. The reaction mixture was then purified as described [25]. The crude product (17.32 g) was purified by flash column chromatography. Fractions were analyzed using Thin-layer Chromatography (TLC) and the product was pooled. The solvent was evaporated, yielding DLin-MeOH (9.7 g, 55%). DLin-MeOH was characterized via ^{1}H-Spectroscopy using a 400 MR-NMR spectrometer (Agilent Technologies, Santa Clara, CA, USA) as shown in Supplementary Fig. S1.

2.1.2. Synthesis of DLin-MC3-DMA

DLin-MC3-DMA was synthesized according to a previously described protocol, with minor modifications [25]. DLin-MeOH (1.32 g, 2.5 mmol) was dissolved in 8 mL of dichloromethane in a 50 mL RB flask. 1-ethyl-3-(3-dimethylaminopropyl) carbodiimide (EDC)*HCL (718 mg, 3.74 mmol), diisopropylamine (0.65 mL) and and 4-dimethylaminopyridine (DMAP) (30 mg, 0.25 mmol) were added. The reaction mixture was stirred for 5 min at room temperature. Dimethylaminobutyric acid (575 mg, 3,43 mmol) was added and stirred overnight at room temperature. Subsequently, the reaction was diluted in dichloromethane (30 mL) and washed with 50% saturated $NaHCO_3$ (20 mL), water (20 mL), and brine (30 mL). The combined organic layers were dried over anhydrous Na_2SO_4 and the solvent was removed in vacuo. The crude product (1.45 g) was then purified using flash column chromatography by a gradient elution form 99.5/0.5 dichloromethane/triethylamine to 97.5/2/0.5 (dichloromethane/methanol/triethylamine) to 96.5/3/0.5 (dichloromethane/methanol/triethylamine). Fractions were analyzed by TLC and pure fractions were pooled and solvent was vacuum evaporated yielding pure Dlin-MC3-DMA (700 mg, 44%) as light-yellow oil. DLin-MC3-DMA was characterized via ^{1}H-Spectroscopy using a 400 MR-NMR spectrometer (Agilent Technologies, Santa Clara, CA, USA) as shown in Supplementary Fig. S2.

2.2. Preparation of modified Cre modRNA

The preparation method of modified Cre modRNA was similar to a previously described protocol [26]. In brief, Cre coding region was amplified by PCR from Cre-IRES-PuroR plasmid (addgene #30205). The backbone of pcDNA3.3-NDG (addgene #26820) without NDG gene was PCR amplified and subsequently assembled with Cre fragment to form pcDNA3.3-Cre using NEBuilder® HiFi DNA Assembly Cloning Kit (New England Biolabs (NEB), Ipswich, MA, USA). After sequencing validation, high purity pcDNA3.3-Cre plasmid was prepared using NucleoBondXtra Maxi kit for transfection-grade plasmid DNA (MACHEREY-NAGEL, Düren, Germany). The pcDNA3.3-Cre plasmid was linearized using *Spe* I to prevent from reading through of the Taq Polymerase. After purification, poly-(A) tail was added by PCR using High-Fidelity hot-start DNA Polymerase (Leishi Bio) according to the manufacture's instruction and the following primers: Primer 1: 5'-TTGGACCCTCGTACAGAAGCTAATACG-3′. Primer 2:T(120)CTTCCTACTCAGGCTTTATT CAAAGACCA. This PCR product was purified and checked by gel electrophoresis. In vitro transcription was carried out by mixing the following items: 3'-O-me-m7G cap analog (6.0 mM, Leishi Bio), GTP (1,5 mM, Leishi Bio), ATP (7,5 mM, Leishi Bio), Me-CTP(7.5 mM, Trilink Biotechnologies, San Diego, CA, USA), Pseudo-UTP(7.5 mM, Trilink Biotechnologies), Tailed PCR template (40 ng/ul) and T7 enzyme and buffer (Veni T7 RNA Synthesis kit, Leishi Bio) and incubated for 4 h in a Thermocycler (Bio-Rad, Hercules, CA, USA). DNA templates were then removed by adding Turbo™ DNase (Thermo Scientific). After cleaning up, modRNA was treated with Antarctic phosphatase (NEB) to remove 5′-triphosphates from the uncapped RNA. After clearing up, the modRNA is aliquoted and stored at −80 °C freezer before use.

2.3. Preparation of LNPs

LNPs were prepared by microfluidic mixing using the NanoAssemblr Benchtop (Precision Nanosystems, Vancouver, Canada). An ethanolic

phase containing lipids was mixed with an acidic aqueous phase (25 mM sodium acetate, pH 4.0) containing modRNA leading to the formation of LNPs. LNPs were produced at a flow rate ratio (aquaous:organic) of 3:1 and a total flow rate of 4.0 mL/min. Cre modRNA was prepared in-house according to the previously decribed procedure. CD70 and firefly luciferase were a gift of eTheRNA Immunotherapies (Niel, Belgium). CD70 mRNA and firefly luciferase mRNA were unmodified, ARCA capped and purified by NaCl precipitation followed by LiCl precipitation. Lipids were dissolved in 100% Ethanol (Merck, Darmstadt, Germany) at a total lipid concentration of 20 mM. The LNPs were composed of DLin-MC3-DMA, Cholesterol (Sigma Aldrich, Saint Louis, MO, USA), DSPC (Lipoid, Ludwigshafen am Rhein, Germany) and PEG-DMG (NOF Corporation, Tokyo, JP) at a molar percentage of 50/38.5/10/1.5, respectively. mRNA/modRNA was encapsulated at a wt/wt ratio (ionizable lipid/RNA) of 10:1. Immediately after production, LNPs were dialyzed against an excess of phosphate buffered saline using Slide-a-Lyzer™ dialysis cassettes G2 with a membrane cutoff of 20 kDa for 16–24 h. After dialysis, LNPs were sterilized using 0.22 μm PVDF membrane filters and concentrated to an appropriate volume using Amicon® Ultra-15 centrifugational filter units with a membrane cutoff of 10 kDa at 2000–4000 rpm at 4 °C. Purified LNP was kept at 4 °C and used within 7 days after production.

2.4. Nanoparticle characterization

2.4.1. Size using dynamic light scattering

The hydrodynamic diameter of LNPs was measured by Dynamic Light Scattering (DLS) using a Zetasizer Nano S (Malvern Panalytical, Malvern, UK) equipped with a 4 mW HeNe laser of 633 nm. Samples were diluted appropriately in Dulbecco's PBS (DPBS) and scattering was measured at an angle of 173° at 37 °C for 10 s and repeated at least 10 times. This procedure was repeated three times for each sample.

2.4.2. Zeta potential

The zeta potential of LNPs was measured using the Zetasizer Nano Z (Malvern Panalytical, Malvern, UK). Prior to analysis LNPs were diluted in 10 mM HEPES (pH 7.4) or 0.1× DPBS (pH 7.4). Each sample was measured at least three times.

2.4.3. RNA determination and determination of encapsulation efficiency

The total RNA concentration was determined using the Quant-It™ Ribogreen RNA Assay kit (Thermo Scientific, Waltham, MA, USA) in the presence of 0.5% (*v*/v) Triton X-100 ($RNA_{tx\text{-}100}$), whereas free/unencapsulated mRNA($RNA_{TE/DPBS}$) was determined in TE or DPBS. The total mRNA/modRNA concentration (μg/mL) or free mRNA/modRNA concentration (μg/mL) was calculated using a reference calibration curve in 0.5% (v/v) Triton-X100 or TE/DPBS buffer. The encapsulation efficiency was then calculated using the following formula (($RNA_{tx\text{-}100}$-$RNA_{TE/PBS}$)/$RNA_{tx\text{-}100}$)*100.

2.5. Animal experiments

2.5.1. Ethical statement on animal experiments

All animal experiments were performed with the Animal Welfare Body Utrecht's permission and complied with the Dutch Experiments on Animals Act (WOD) under license AVD115002015257. The research was carried out in accordance with the Guide for the Care and Use of Laboratory Animals.

2.5.2. Myocardial infarction and reperfusion

The left anterior descending coronary artery (LAD) was ligated for 60 min before reperfusion was induced to induce myocardial ischemia and reperfusion injury. Briefly, mice were anesthetized with fentanyl (0.05 mg/kg), midazolam (5 mg/kg) and medetomidine (0.5 mg/kg) by intraperitoneal injection. Surgical procedures were performed minimally invasive and under sterile conditions. Hearts were exposed by creating an opening between 3rd and 4th ribs and the LAD was ligated below the left atrial appendage with an 8–0 Ethilon monifil suture. After 60 min, the ligature was carefully removed to start reperfusion. After the chest was closed, anesthesia was antagonized (with atipamezole (2.5 mg/kg) and flumazenil (0.5 mg/kg)) and supplemented with Temgesic (0.1 mg/kg) for quick recovery and pain relief. Analgesia was given every 12 h after surgery for two days. At the end of each experiment, mice were terminated with overdose anesthesia with i.p. sodium pentobarbital 60 g/kg.

2.5.3. In-vivo circulation time and bio-distribution of LNP-modRNA after Myocardial Infarction

The biodistribution of LNPs encapsulating modRNA was assessed in 22 female C57Bl/6 mice ($N = 22$, weight between 22 and 25 g, 12 week old, Charles River, Leiden, the Netherlands) with the use of fluorescently labeled LNPs (0.2 mol% DSPE – Cy5.5). Two mice died consequential to the MI surgery and as such they were excluded from the study. Animals were divided in 3 experimental groups: Animals in group 1 ($N = 8$) underwent myocardial ischemia-reperfusion, animals in group 2 (N = 8) were sham-operated animals and animals in group 3 ($N = 4$) were control animals for background analysis of fluorescence. Sixty minutes after reperfusion, a dose of 50 μg LNP encapsulated modRNA was administered intravenously (i.v.) via the tail vein. Per animal, blood was collected at 3 pre-defined time points. Blood was collected either at $t = 1$ min, 30 min and 240 min ($N = 4$) or at t = 1 min, 2 h and 24 h (N = 4). For control animals, the group size $N = 2$. Blood was withdrawn via tail vein ($T = 1$ min, 30 min, 2 h) or heart puncture ($t = 240$ min or 24 h) and collected in EDTA anti-coagulated tubes. Blood samples were stored on ice and then centrifuged for 10 min at 2000 x*g* and 4 °C. Platelet-poor plasma was collected and stored at −80 °C until further analysis.

At the end of each experiment, mice were terminated with overdose anesthesia with i.p. sodium pentobarbital 60 g/kg after 240 min (N = 4) or 24 h (N = 4) (Fig. 2A). Then, the mice were perfused with PBS via the left ventricle cavity. Organs were collected and tissue distribution of the LNPs was immediately analyzed by measurement of fluorescence signal using a Pearl Impulse Imager (Li-cor Biosciences, Lincoln, NE, USA). After imaging, organs were snap-frozen in liquid nitrogen and stored at −80 °C until further analysis. Fluorescence in plasma and tissue lysates was analyzed by fluorescent spectroscopy on a Spectramax ID3 (Molecular Devices, San Jose, California, USA) at excitation/emission wavelengths of 675/720 nm, respectively. Plasma samples were first diluted 3× in Dulbecco's PBS; then 25 μL of diluted platelet free plasma was transferred to a black 384 well plate and measured. Data is expressed as % of the value obtained at $t = 1$ min. Tissue lysates were obtained from liver, spleen, lungs, a single femur, a single kidney, and the whole heart. Organs were weighed, transferred to a 2 mL tube containing ceramic beads (1.4 mm) and 3 μL of RIPA-buffer was added for every milligram of tissue. Tissues were homogenized using a Mini bead-beater 8 (Biospec, Bartlesville, OK, USA) for 60 s. Samples were centrifuged for 10 min at 10.000 *g* and 4 °C. 25 μL of supernatant was transferred to a black 384 well plate and fluorescence was measured.

2.5.4. Functional Delivery of firefly luciferase mRNA after myocardial infarction

The efficacy of LNPs delivering luciferase mRNA was assessed after myocardial infarction by measurement of the luciferase activity 4 h after administration. For this experiment, Ai9 mice (the Jackson laboratory, No: 007909) were used and received standard chow and water ad libitum. LNPs were administered at a single dose of 50 μg mRNA/animal 1 h after the start of the reperfusion ($N = 4$). As a control group, we used sham-operated mice(N = 4). C57Bl/6 mice were used as blanks ($N = 2$). Mice were sacrificed 4 h post-injection and were perfused using 7 mL of PBS (Fig. 3A). Tissues were directly snap-frozen and stored at −80 °C until further processing. Luciferase activity was measured in tissue lysates. Tissues were weighed, transferred to a 2 mL tube containing ceramic beads(1.4 mm) and 5 μL of Cell Culture Lysis Reagent was added

for every milligram of tissue (Promega, Leiden, NL). Tissues were homogenized using a Mini bead-beater for 60 s. Samples were centrifuged for 10 min at 10000 *g* and 4 °C. The supernatant was transferred to a fresh tube. Samples were stored at −80 °C until further analysis. Luciferase activity was measured using the Spectramax ID3 with the injector (Molecular Devices, San Jose, California, USA). 10 μL of supernatant was added to a white 96 well plate (Greiner,). 50 μL of Luciferase Assay Reagent (Promega, Leiden, Netherlands) was dispensed using the injector under shaking, incubated for 2 s and luminescence was measured at an integration time of 10 ms.

2.5.5. Functional delivery of Cre recombinase modRNA after myocardial infarction

The dose-dependent cell-type-specific uptake of LNP modRNA after myocardial infarction was investigated by microscopic study of tdTomato+ cells seven days after i.v. administration of LNP/Cre modRNA. Eighteen 12-week old Ai9 mice (Jackson Laboratory, Bar Harbor, ME, USA, No: 007909) were operated on to induce myocardial infarction as described above. After the mice are recovered from anesthesia, mice were divided into six groups, three per group and injected with a single dose of LNPs containing 0 μg, 5 μg, 10 μg, 25 μg, 50 μg and 100 μg of Cre modRNA, respectively. The mice returned to standard housing with a warming pad and were terminated seven days post-injection.

3. Histology

Tissues (heart, lungs, kidney, spleen and liver) were collected, fixed and embedded in paraffin blocks. 3 μm Paraffin sections were prepared with a microtome (Leica, RM2235). Antigen retrieval was performed with a pressure cooker method with citrate buffer (pH 6.0). Immunofluorescent staining was performed with the following primary and secondary antibodies: Anti-RFP (Rockland Immunochemicals, cat. # 600–401-379, 1:500), Mac3 (BD Bioscience, cat. # BDB553322, 1:100), anti-CD45(eBioscience, cat. # 30-F11, 1:100), FITC-labeled MF20 (Developmental Studies Hybridoma Bank, 1:500,), αSMA (Sigma-Aldrich, Cat.# A2547, 1:200), Donkey anti-Rabbit IgG (H + L) Highly Cross-Adsorbed Secondary Antibody Alexa Fluor 555 secondary antibody (Thermo-Fisher Scientific, Cat. # A-31572, Dilution) was used to visualize the primary anti-RFP antibody. Donkey anti-Rat IgG (H + L) Highly Cross-Adsorbed Secondary Antibody Alexa Fluor 488 (Thermo Fisher Scientific, Cat # A-21208, Dilution) was used to visualize Rat primary antibody. The whole tissue section was scanned with NanoZoomer S360 Digital slide scanner (Hamamatsu Photonics K·K, Hamamatsu Japan) and analyzed with NDP.view2 Viewing software: U12388–01 (Hamamatsu Photonics K·K, Hamamatsu Japan), to gain the overall distribution of the targeted cells in the whole tissue section. The liver toxicity was evaluated using H.E. staining and examined by an experienced pathologist.

4. Statistical analysis

Statistical analysis was performed using GraphPad Prism v8.3 (Graphpad Software, San Diego, CA, USA). Tissue distribution of fluorescent LNPs and luciferase mRNA expression were analyzed per organ using an unpaired students *t*-test. Differences in plasma concentration of LNPs was analyzed per time point using an unpaired students t-test. A result was statistically significant if $P < 0.05$.

5. Results

5.1. Particle characterization

Three different LNPs were produced by microfluidic mixing using the NanoAssemblr Benchtop device: LNPs encapsulating firefly luciferase mRNA, and LNPs containing Cre recombinase modRNA (Fig. 1A and B). The size of all particles was below 100 nm at a PDI <0.2. Incorporation of a fluorescent lipid, 0.2% DSPE-Cy5.5, in LNPs did not affect particle characteristics (Fig. 1C). The batch-to-batch variability in terms of size

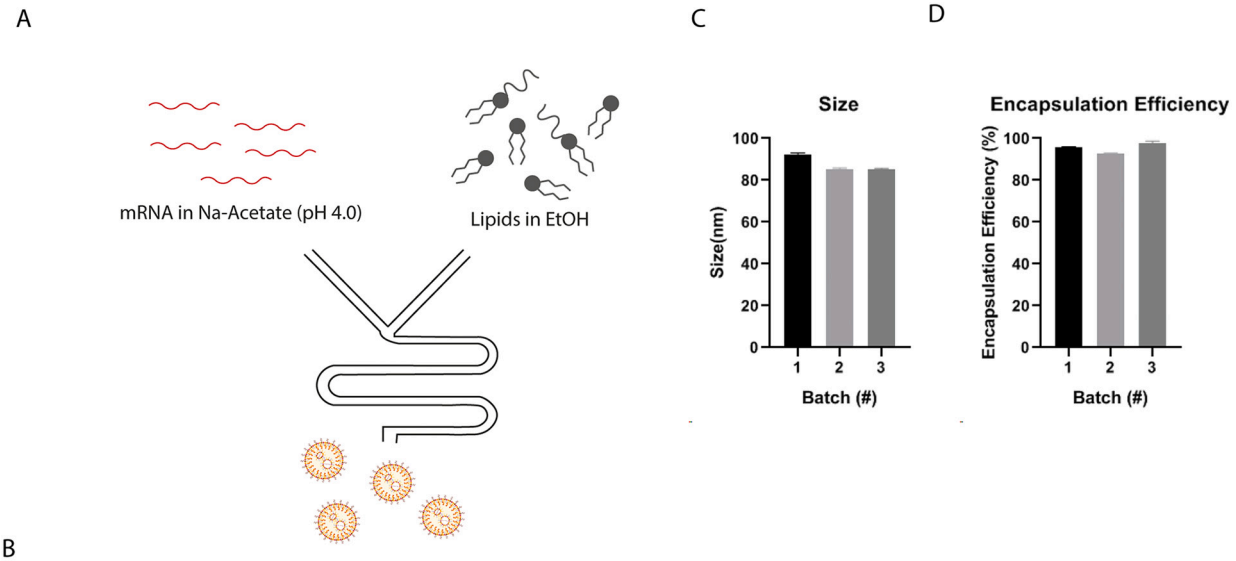

B

Formulation	Components	Particle size(nm)	PDI	Zeta Potential (mV)	mRNA Encapsulation(%)	Batches
fLNP-mRNA	DLin-MC3-DMA/Cholesterol/DSPC/DMG-PEG2000/DSPE-PEG-Cy5.5 = 50/38,3/10/1,5/0,2	74	0,13	-4,2	98,6	1
LNP-mRNA fLuc	DLin-MC3-DMA/Cholesterol/DSPC/DMG-PEG2000 = 50/38,5/10/1,5	69	0,07	-4,8	98,0	1
LNP-mRNA Cre	DLin-MC3-DMA/Cholesterol/DSPC/DMG-PEG2000 = 50/38,5/10/1,5	87	0,10	-7,9	95,4	3

Fig. 1. Production and Characterization of LNPs.
A) Schematic Illustration of LNP production using microfluidic mixing. B) Tabular overview of LNP formulations and particle characteristics. Mean values of particle size (z-average), polydispersity index, z-potential, and encapsulation efficiency are reported. n = 3C) Batch to batch size variability. Three separate batches of LNP-modRNA Cre were produced over a period of 1 year. Z-average is reported as size; Mean ± SD. D) Batch-to-batch variability of encapsulation efficiency. n = 3.

and encapsulation efficiency between various LNP batches are shown in Figs. 1D and E. The observed formulation characteristics of LNPs correspond well with particles of similar composition, reported previously [27,28].

5.2. In-vivo biodistribution after ischaemia reperfusion injury shows increased accumulation in the infarcted area of the heart

LNPs were fluorescently labeled using 0.2 mol% DSPE-Cy5.5 to allow the analysis of tissue distribution using fluorescent imaging and fluorescence quantification. Fluorescently labeled LNPs (fLNPs) were administered 1 h after the start of reperfusion in a murine ischemia-reperfusion model and blood samples were taken at $t = 1$ min,30 min,60 min, 240 min and 24 h post-injection. Fluorescence in plasma samples was determined and expressed as a percentage of the fluorescence measured directly after injection (t = 1 min). Fig. 2 shows that the majority of fLNPs were removed from circulation within 4 h upon injection (Fig. 2E). The ischemia-reperfusion injury did not influence fLNP plasma concentrations at any of the measured time points and no differences in blood plasma concentrations as measured by the fluorescence in blood plasma were observed between sham-operated and ischemia-reperfusion mice.

Directly after euthanasia, animals were perfused using PBS, whole organs were resected, and fluorescent tissue distribution imaged on a Pearl® Small Animal Imaging System. Imaging of indicated organs showed the accumulation of fLNPs in the heart upon ischemia-reperfusion 4 h after administration (Fig. 2B). fLNPs mainly accumulated in the infarcted area just below the region where the left anterior descending artery was occluded. We did not observe any accumulation of LNPs in the heart of sham-operated or control animals. Differences in tissue distribution were still seen after 24 h but overall myocardial and tissue fluorescence decreased (Fig. 2B). Taken together, upon ischemia-reperfusion injury, fLNP accumulated in the infarcted area of the heart.

Additionally, fluorescence levels were measured in tissue homogenates to quantify the amount of fluorescence in the organs. As indicated in Figs. 2C and D, total fluorescence in the heart was increased in the ischemia-reperfusion injury group compared to the sham-operated group both at 4 and 24 h. No differences were found in other organs. Both fluorescent imaging of whole organs and quantification of fluorescence in tissue lysates indicated an increased accumulation of LNPs in cardiac tissue after ischemia-reperfusion injury. However, the intensity of the fluorescent signal was relatively low compared to organs such as the liver and spleen.

5.3. Administration of LNPs-mRNA after ischemia-reperfusion injury results in increased cardiac mRNA expression

To explore whether the increased accumulation of LNPs also affected the functional expression patterns of mRNAs, we intravenously injected LNP containing 50 μg of firefly luciferase mRNA 1 h after the start of reperfusion and compared luciferase activity to the group of sham-operated mice. Fig. 3 shows that myocardial luciferase activity in the ischemia-reperfusion injury group was significantly increased compared to the sham-operated control group. As expected from previous observations, cardiac luciferase activity was relatively low compared to organs in which LNPs typically accumulate, such as the liver and the spleen.

5.4. LNPs-modRNA deliver modRNA to cells in the infarcted area of the heart, mainly αSMA+ cardiac fibroblasts

Different cell types play distinct roles in the pathological development of heart failure and therapeutic intervention can only achieve a maximum effect if the therapy reaches the desired organ region and cell type [29–31]. To assess functional delivery of LNPs and identify the cells targeted, Cre/loxP reporter Ai9 mice were systemically injected with different doses of LNPs encapsulating Cre modRNA. In these mice, functional delivery of Cre recombinase modRNA results in Cre-mediated recombination, excising the STOP cassette, leading to the expression of tdTomato. Upon injection of a single dose of LNP-modRNA, we observed a dose-dependent increase of tdTomato+ cells in the heart as well as in the other organs, as shown in Fig. 4 and Supplementary Fig. 3. In the heart, we noticed that most of the tdTomoto+ cells were located in the infarcted area, but at higher doses (above 50 μg/mice), cells in the pericardial layer also became positive (Fig. 4). We performed immunofluorescence staining with different cell-specific markers to identify these tdTomato+ cell types in the infarct area. Most of the tdTomato+ cells were identified as fibroblasts (αSMA+), whereas some tdTomato+ cardiomyocytes and macrophages could also be observed (Fig. 5). In an independent experiment, we compared naked Cre modRNA with LNP encapsulated Cre modRNA in sham and MI operated animals. Here, we observed that naked Cre RNA injection resulted in only a low number of tdTomato+ cells (Supplementary Fig. 4). To exclude liver toxicity by the use of the high doses of LNP-modRNA we performed H&E staining on the animals that were treated with high doses of LNP-modRNA (above 50 μg modRNA). Pathological examination revealed no difference compared with PBS controls, even at the highest dose (100 μg) used (supplementary fig. 5).

6. Discussion

This study explored the feasibility of functional mRNA/modRNA delivery to the myocardium after myocardial infarction using LPNs. modRNA therapy holds great promise in cardiac regeneration therapy. However, its functional delivery is challenged by the physicochemical properties of the RNA molecule including its size and charge limiting it's cellular uptake and release into the cytosol. Here, we explored the feasibility of lipid nanoparticles as a carrier for both modified and unmodified RNA to enable functional delivery to the myocardium via an intravenous route. After *i.v.* administration, LNPs accumulated in the ischemic region of the heart after ischemia-reperfusion injury. More importantly, increased tissue accumulation of LNP-modRNA led to increased functional protein production in the heart compared to sham-operated animals.

Tissue distribution of LNPs encapsulating modRNA to the ischemic area of the myocardium was not unexpected given the literature available on the administration of lipid nanoparticles after myocardial infarction [23,24]. Ischemia-reperfusion injury leads to increased vascular permeability enabling extravasation of nanoparticles. This resulted in a clear increase in accumulation of LNPs in the heart after ischemia-reperfusion injury as observed by whole-organ fluorescent imaging and the measurement of fluorescence in tissue lysates. However, the measurement of LNP tissue biodistribution by fluorescent labeling of LNPs is not without its drawbacks. Firstly, labeling of the nanoparticle with a fluorescent lipid provides no data on the distribution of the actual therapeutic component: modRNA. Besides, previous reports have shown that fluorescent lipid probes can dissociate from PEGylated liposomes in a biological environment over a time course of 24 h [32]. Secondly, the quantitative data obtained via in vivo imaging of fluorescent nanoparticles may be influenced by quenching by blood components as well as differences in light scattering between organs [33,34]. This study took all of these considerations into accounts. Diffusion of the PEG-lipid is expected to have limited influence since circulation half-time of the LNPs is expected to be ±30 min. Organs were perfused with PBS prior to measurement to reduce possible interference of blood components. Apart from whole-organ imaging, fluorescence in tissue lysates was also analyzed to account for the eventual influence of light scattering on the results. Moreover, the functional bio-distribution of modRNA was evaluated by measurement of luciferase activity after administration of LNPs encapsulating firefly luciferase modRNA.

The increased delivery of LNP-mRNA to the infarcted heart also led to an increase in functional protein production of luciferase mRNA in IR-

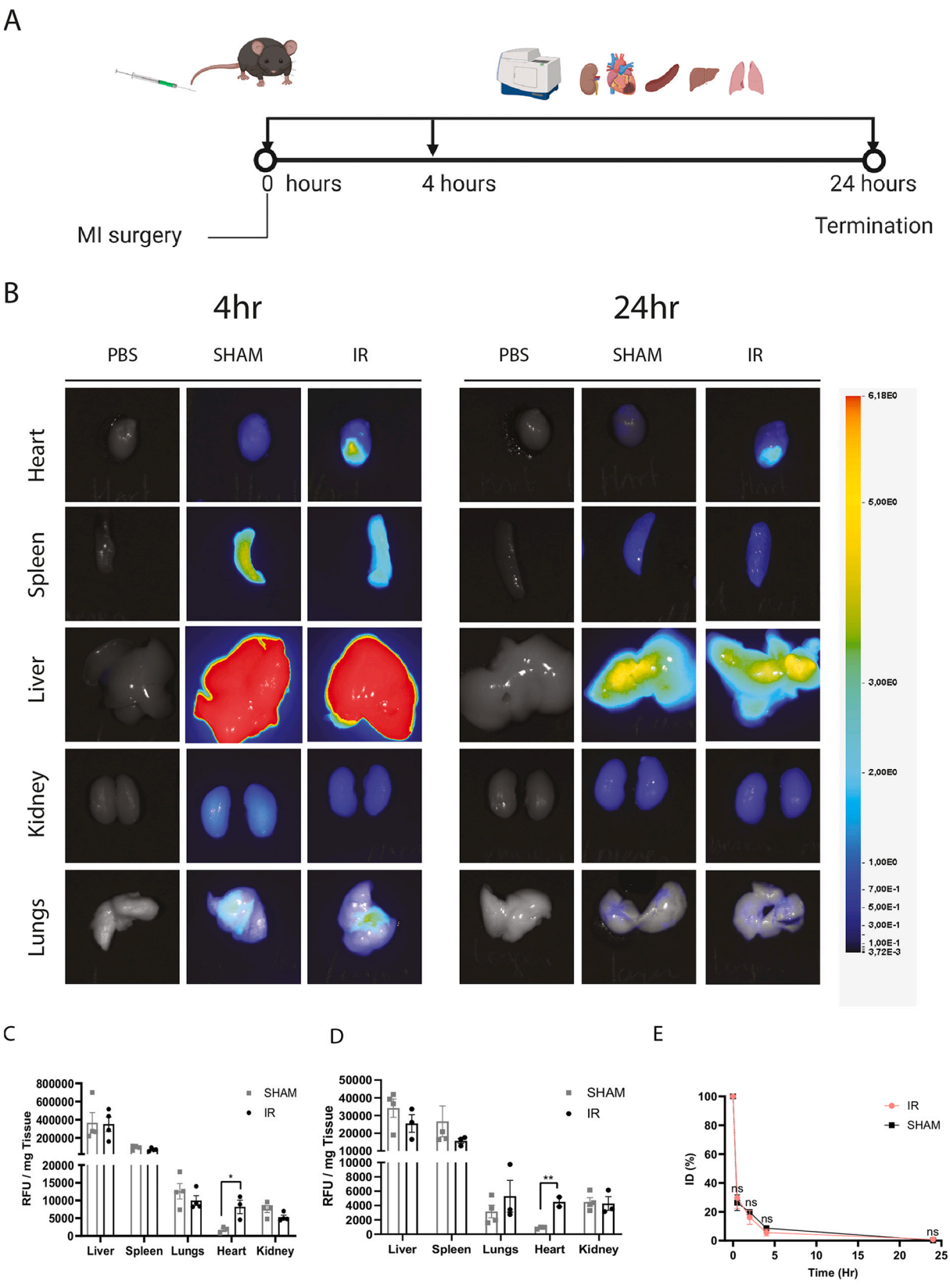

Fig. 2. Biodistribution of fLNP-mRNA after sham-operation or ischemia-reperfusion injury.
LNP-mRNA wasadministered at a dose of 50 μg mRNA to either sham-operated or ischemia-reperfusion injury animals. Mice were sacrificed after 4 or 24 h. A) Experimental design of the biodistribution study. B) Biodistribution of fluorescently labeled LNPs was measured by whole-organ fluorescence spectroscopy. Representative fluorescence/brightfield overlay images of murine organs harvested 4 and 24 h after injection with 50 μg LNP-mRNA. Tissue distribution of fLNP after 4 h (C) or 24 h (D) as determined by ex vivo luminescence of tissue lysates . Bars show mean RFU ± SD, n = 4. E) Plasma concentration of fLNPs over time. Plasma concentration is expressed as a percentage of the plasma fluorescence directly measured after injection (t = 1 min). n = 4–8; mean ± SD. * represents $P < 0,05$. ** represents $P < 0,01$.

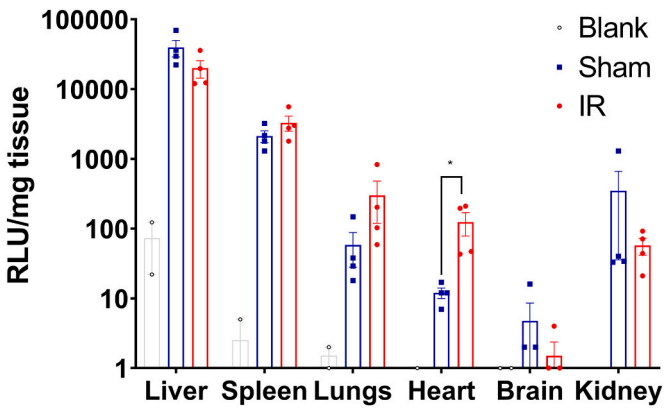

Fig. 3. Luciferase activity in different organs lysates 4 h after LNP-mRNA fLuc administration.
Luciferase activity in homogenates of different organs 4 h after intravenous administration of 50 μg firefly luciferase mRNA encapsulated in LNPs. LNPs were administrated 1 h after reperfusion of mice. Luciferase activity per mg tissue is plotted on a logarithmic scale. The untreated animals are C57/Bl6 mice without any treatment providing a background signal in different organs. N = 2–4. * represents $P < 0,05$.

animals compared to a control group. In all other organs, no significant difference in luciferase activity was observed between sham and ischemia-reperfusion operated animals, typically observed for nanoparticles when administered intravenously [35]. Although LNP distribution and protein expression is increased in the heart after IR-injury by taking advantage of damage-induced vascular permeability phenomena, luciferase activity is still relatively low compared to the liver and spleen. Therefore, it would be interesting to study the timeframe of vascular leakage after myocardial infarction and determine at what time point within that timeframe is the most optimal time point for the injection of LNPs to improve the balance between on- and off-target delivery. For stable, chronic heart failure patients without myocardial infarction, the access of LNPs through vascular leakage will not occur. Here, pretreatment with ultrasound-induced microbubble-destruction to induce local vascular permeability might be helpful [36]. Liver and splenic mRNA expression can also be attenuated by the incorporation of microRNA binding domains in the 3'-UTR of mRNA. Jain et al. showed that the incorporation of miR-122 binding sites in the 3'UTR led to diminished expression of mRNA in liver hepatocytes [28] When miR-142 binding sites were incorporated, splenic mRNA expression was reduced [28]. Such an approach can be used to reduce the systemic translation of a protein, thereby reducing the risk of side effects in non-targeted organs. The biodistribution of LNP/mRNA can be affected by through optimization of the LNPs' lipid composition. For instance, Dahlman et al. have shown that variations in the structure of the PEG-lipid influences tissue distribution and that incorporation of different PEG-lipids can lead to increased accumulation in the heart [37]. Another potential approach to alter the expression pattern of the mRNAs using LNP is via the targeting approach. Recently, Peer's group has developed a self-assembly platform with an Fc domain anchored to the surfaced of LNP which can be easily combined with mAbs to target any cell type of interest. In addition, an increasing number of infarct specific genes have been identified, the development of binders such as mAb and nanobodies will be very helpful to develop myocardial infarction enhanced delivery of LNP in

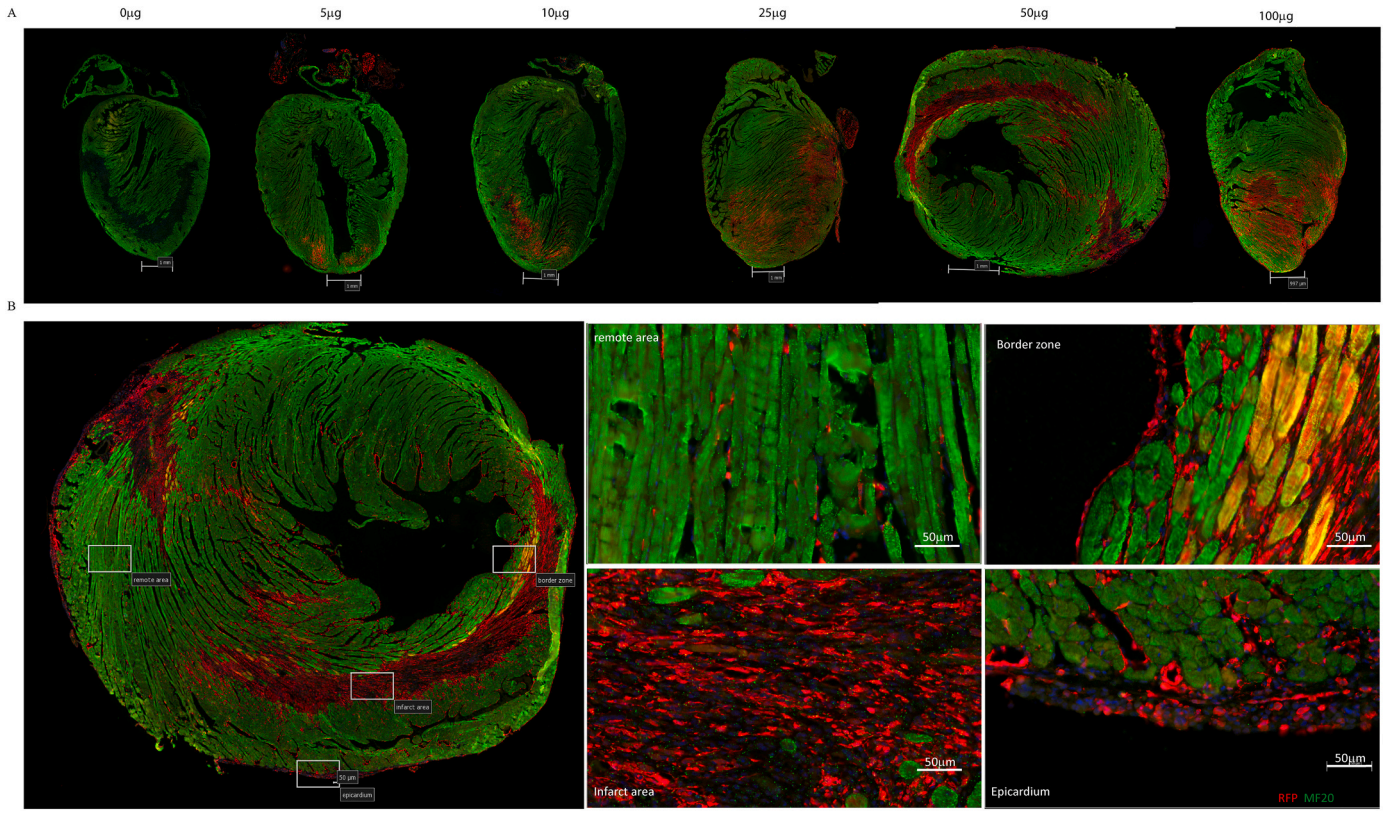

Fig. 4. Dose-dependent delivery of LNP-encapsulated Cre modRNA to the infarcted myocardium. A) A bird's-eye view of tdTomato+ cells at the different doses. tdTomato was stained with anti-RFP antibody in red, cardiomyocytes were stained using the MF20 antibody in green and Hoechst in blue. Note, the absence of green signal within myocardium indicated the infarcted areas. The scalebar represents 1 mm. B. Identification of different locations within the heart. Infarct Area; Border Zone; Remote Area and epicardium. On the right, a zoom-in of tdTomato+ cells at different locations within the heart is shown. Orange cells in D indicate tdTomato+ cardiomyocytes which are stained positive in both red and green. Images were taken with NanoZoomer S360 Digital slide scanner and digitally magnified 20 times. The scalebar represents 50 μm. (For interpretation of the references to colour in this figure legend, the reader is referred to the web version of this article.)

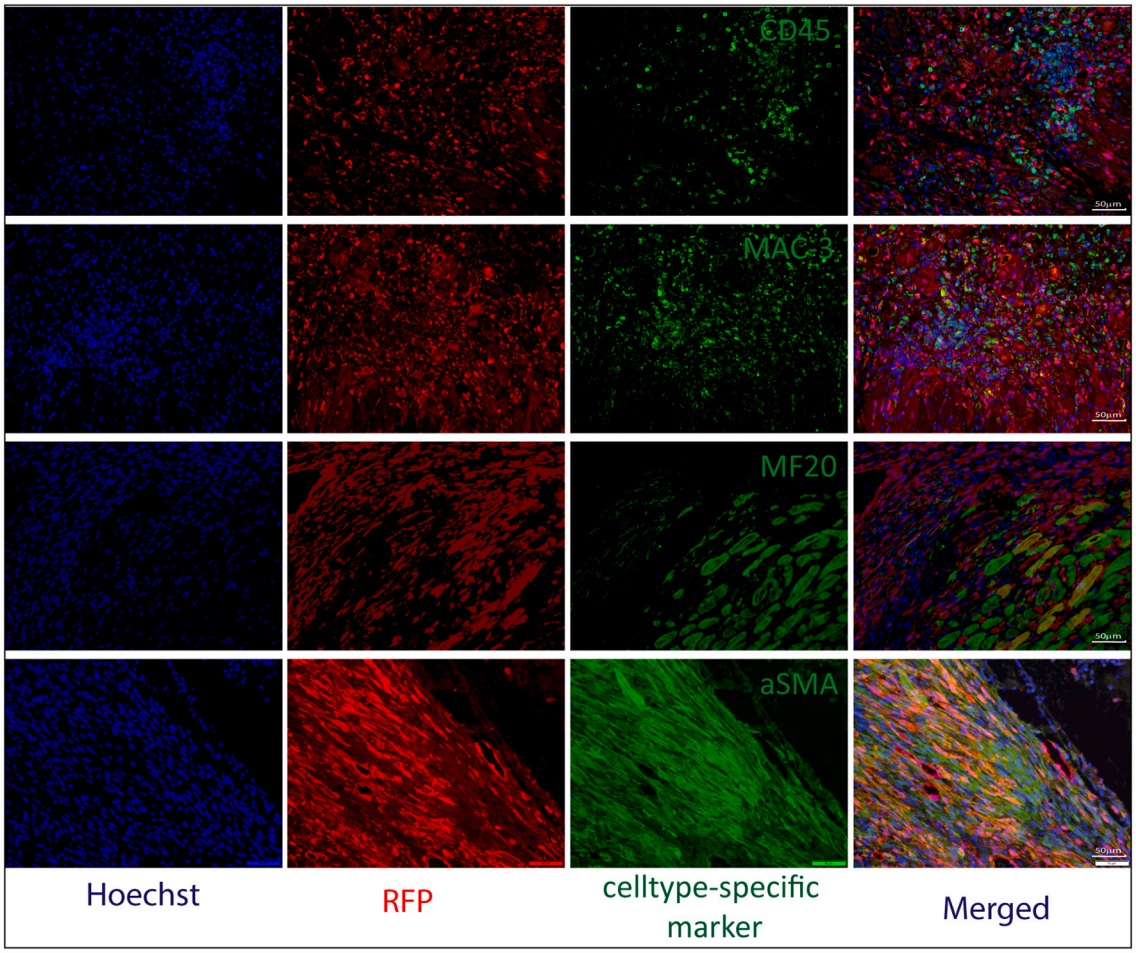

Fig. 5. Characterization of Tdtomato + cells after Cre modRNA delivery to the infarcted area of the myocardium. tdTomato was stained with anti-RFP in red, and co-stained with cell-type-specific markers CD45 (Leukocytes), MAC-3 (macrophages), MF20 (cardiomyocytes), and αSMA(fibroblasts) in green. Note, only small number of Mac-3^{+} and MF20^{+} cells were also tdTomato+, most of the tdTomato+ cells were fibroblasts. Nuclei were visualized with Hoechst 33342 in blue. The scalebar represents 50 µm. (For interpretation of the references to colour in this figure legend, the reader is referred to the web version of this article.)

the future.

Therapeutic use of modRNA in cardiac disease was already explored by others, albeit via other administration routes and/or mRNA drug delivery systems [20,21,38–44]. Most reported alternative administration routes are either direct intramyocardial injection or intraventricular injection with temporary aortic cross clamping. Compared to I.V. administration, these administration routes are more invasive. However, certainly for direct intramyocardial injection, the expression profile of the modRNA may be more localized in the heart with lower expression levels observed in spleen and liver which might be considered as an advantage [45]. Most interestingly, modRNA can also be functionally delivered to the heart via direct intracardiac injection in saline, citrate-saline buffer or a sucrose-citrate buffer with varying efficacy [44]. Functional delivery of naked modRNA, without an additional drug delivery vehicle, is only feasible in the heart, skin and skeletal muscle with no expression observed in liver, kidney and pancreas [38]. It is hypothesized that the modRNA is located along the cardiac sarcolemma providing a modRNA reservoir protecting the modRNA from RNAses. However, the exact mechanism of modRNA uptake and more interestingly the release of modRNA from the *endo*-lysosomal system to the cytosol is yet to be revealed. Currently, the high doses (100–150 µg modRNA per injection) used in functional studies might limit clinical translation due to the high dose associated costs and might warrant further investigation into lipid based drug delivery vehicles to enhance modRNA delivery to the heart.

Different cell types play distinct roles during the development of heart failure after myocardial infarction and therapeutic intervention can only achieve maximum effect if the desired therapy reaches the targeted cell type [4,29–31,46]. Therefore, it was of interest to evaluate which cell types in the myocardium were transfected by LNP-modRNA. Cre reporter mice gave us a possibility to precisely measure which cell types have taken up the LNP encapsulated Cre modRNAs using FACS or single cell sequencing technology. However, it turned out to be technically very challenging in the infarcted heart. The infarct scar is composed of fibrotic tissue which is very difficult to digest enzymatically. As a consequence, the cell types which are prone to be single cells such as T cells, B cells will be over-represented in the final results cardiomyocytes and fibroblasts, which are sensitive to cell isolation procedures, will be underrepresented. Therefore, we decided to use the fluorescent microscopy approach which provides the spatial location of the cells that have taken up the LNP within the infarct myocardium even though it compromised in terms of quantification of the number of cells that have taken up the LNPs. Upon administering LNPs encapsulating Cre Recombinase modRNA to Cre-LoxP reporter mice, we observed that LNPs transfected cells both in the infarct region as well as the pericardial layer. Within the infarction area, the most efficiently targeted cell type was the cardiac fibroblast, which plays an important role in the development of cardiac fibrosis and during the remodeling phase in the heart [47]. The targeted delivery of therapeutic modRNA to these fibroblasts might be beneficial in two different potential therapeutic strategies. Firstly, it may be exploited to reduce the development of cardiac fibrosis directly [29]. Secondly, given the recent development in the

aforementioned cardiac reprogramming technology, it can also be used to convert cardiac fibroblasts into cardiomyocytes directly [48,49]. It must also be taken into account that the Cre-LoxP model is a very sensitive approach and given its binary "on/off'" nature, no data is obtained about the expression levels of the delivered modRNA in cardiac fibroblasts and whether or not this is sufficient to reach therapeutic concentrations.

These data suggest that LNPs encapsulating modRNA might be an alternative to various delivery methods currently used for reprogramming cardiac fibroblast to cardiomyocytes or for the expression of therapeutic proteins via plasmid DNA. Moreover, the delivery of LNPs encapsulating modRNA is also an alternative for recombinant protein administration [50].

7. Conclusion

The results presented here demonstrate the feasibility of functional modRNA delivery by LNPs to the infarct region after myocardial infarction. Given the rapid progress in the cardiac regeneration field, an approach using LNPs to deliver modRNA might accelerate the translation of newly identified pro-cardiac regeneration genes into the clinic.

CRediT authorship contribution statement

Martijn J.W. Evers: Investigation, Writing – original draft. **Wenjuan Du:** Investigation, Writing – original draft. **Qiangbing Yang:** Investigation. **Sander A.A. Kooijmans:** Investigation. **Mies van Steenbergen:** Investigation. **Pieter Vader:** Funding acquisition, Supervision. **Saskia C.A. de Jager:** Funding acquisition, Resources. **Enrico Mastrobattista:** Resources. **Joost P.G. Sluijter:** Conceptualization, Funding acquisition, Supervision. **Zhiyong Lei:** Conceptualization, Investigation, Writing – original draft. **Raymond Schiffelers:** Conceptualization, Funding acquisition, Supervision.

Acknowledgment

We would like to thank Maike Brans and Domenico Castigliego for their technical assistance and Dr. Daniel Murphy for proof reading of the manuscript. Wenjuan Du is supported by a postdoc fellowship from Chinese Research Council and Chunhui Project (HLJ2019014). This work is supported by the European Union's Horizon 2020 Research and Innovation Programme in the project B-SMART (to P·V. and R.M.S.) under grant agreement No. 721058, by Netherlands Organization for Scientific Research (NWO) Technical and Applied Sciences Domain High Tech Systems and Materials Programme in the project TORNADO under grant agreement No. 16169 (To R. M.S), by Horizon 2020 Research and Innovation Programme in the project EXPERT under grant agreement No. 825828 (To P. V, and R.M.S).This work is also supported by the Project EVICARE (No. 725229) of the European Research Council (ERC) to J.P.G.S., co-funded by the Project SMARTCARE II of the Bio-MedicalMaterials institute to J.P.G.S., the ZonMw-TAS program (No. 116002016) to J.P.G.S./Z.L., PPS grant (No. 2018B014) to J.P.G.S./P.V/Z.L, the Dutch Ministry of Economic Affairs, Agriculture and Innovation and the Netherlands CardioVascular Research Initiative (CVON): the Dutch Heart Foundation to J.P.G.S., Dutch Federations of University Medical Centers, the Netherlands Organization for Health Research and Development, and the Royal Netherlands Academy of Sciences. P.V. acknowledges support from the Dutch Heart Foundation (Dr. E. Dekker Senior Scientist grant, # 2019T049).

Appendix A. Supplementary data

Supplementary data to this article can be found online at https://doi.org/10.1016/j.jconrel.2022.01.027.

References

[1] C.W. Yancy, M. Jessup, B. Bozkurt, J. Butler, D.E. Casey, M.M. Colvin, M. H. Drazner, G.S. Filippatos, G.C. Fonarow, M.M. Givertz, ACC/AHA/HFSA focused update of the 2013 ACCF/AHA guideline for the management of heart failure: a report of the American College of Cardiology/American Heart Association Task Force on Clinical Practice Guidelines and the Heart Failure Society of America, J. Am. Coll. Cardiol. 70 (2017) (2017) 776–803.
[2] M.A. Laflamme, C.E. Murry, Heart regeneration, Nature 473 (2011) 326–335.
[3] L. de Wit, J. Fang, K. Neef, J. Xiao, Pieter A. Doevendans, Raymond M. Schiffelers, Zhiyong Lei, Joost P.G. Sluijter, Cellular and molecular mechanism of cardiac regeneration: a comparison of newts, Zebrafish Mammals Biomol. 10 (2020).
[4] Q. Yang, J. Fang, Z. Lei, J.P.G. Sluijter, R. Schiffelers, Repairing the heart: state-of the art delivery strategies for biological therapeutics, Adv. Drug Deliv. Rev. 160 (2020) 1–18.
[5] Z. Lin, A. von Gise, P. Zhou, F. Gu, Q. Ma, J. Jiang, A.L. Yau, J.N. Buck, K.A. Gouin, P.R. van Gorp, Cardiac-specific YAP activation improves cardiac function and survival in an experimental murine MI model, Circ. Res. 115 (2014) 354–363.
[6] A. von Gise, Z. Lin, K. Schlegelmilch, L.B. Honor, G.M. Pan, J.N. Buck, Q. Ma, T. Ishiwata, B. Zhou, F.D. Camargo, YAP1, the nuclear target of hippo signaling, stimulates heart growth through cardiomyocyte proliferation but not hypertrophy, Proc. Natl. Acad. Sci. 109 (2012) 2394–2399.
[7] M. Xin, E.N. Olson, R. Bassel-Duby, Mending broken hearts: cardiac development as a basis for adult heart regeneration and repair, Nat. Rev. Mol. Cell Biol. 14 (2013) 529–541.
[8] K. Bersell, S. Arab, B. Haring, B. Kühn, Neuregulin1/ErbB4 signaling induces cardiomyocyte proliferation and repair of heart injury, Cell 138 (2009) 257–270.
[9] G. D'Uva, A. Aharonov, M. Lauriola, D. Kain, Y. Yahalom-Ronen, S. Carvalho, K. Weisinger, E. Bassat, D. Rajchman, O. Yifa, ERBB2 triggers mammalian heart regeneration by promoting cardiomyocyte dedifferentiation and proliferation, Nat. Cell Biol. 17 (2015) 627–638.
[10] K. Harada, M. Friedman, J. Lopez, S. Wang, J. Li, P. Prasad, J. Pearlman, E. Edelman, F. Sellke, M. Simons, Vascular endothelial growth factor administration in chronic myocardial ischemia, Am. J. Phys. Heart Circ. Phys. 270 (1996) H1791–H1802.
[11] S.L. House, C. Bolte, M. Zhou, T. Doetschman, R. Klevitsky, G. Newman, J.E. J. Schultz, Cardiac-specific overexpression of fibroblast growth factor-2 protects against myocardial dysfunction and infarction in a murine model of low-flow ischemia, circulation 108 (2003) 3140–3148.
[12] M. Simons, B.H. Annex, R.J. Laham, N. Kleiman, T. Henry, H. Dauerman, J. E. Udelson, E.V. Gervino, M. Pike, M. Whitehouse, Pharmacological treatment of coronary artery disease with recombinant fibroblast growth factor-2: double-blind, randomized, controlled clinical trial, circulation 105 (2002) 788–793.
[13] K. Miyamoto, M. Akiyama, F. Tamura, M. Isomi, H. Yamakawa, T. Sadahiro, N. Muraoka, H. Kojima, S. Haginiwa, S. Kurotsu, Direct in vivo reprogramming with Sendai virus vectors improves cardiac function after myocardial infarction, Cell Stem Cell 22 (2018) (91–103. e105).
[14] K. Song, Y.J. Nam, X. Luo, Heart repair by reprogramming non-myocytes with cardiac transcription factors[J], Nature 485 (7400) (2012) 599–604.
[15] C.E. Thomas, A. Ehrhardt, M.A. Kay, Progress and problems with the use of viral vectors for gene therapy, Nat. Rev. Genet. 4 (2003) 346–358.
[16] B. Meibohm, Pharmacokinetics and half-life of protein therapeutics, Therapeutic proteins: strategies to modulate their plasma half-lives 48, 2012.
[17] K. Kariko, H. Muramatsu, J. Ludwig, D. Weissman, Generating the optimal mRNA for therapy: HPLC purification eliminates immune activation and improves translation of nucleoside-modified, protein-encoding mRNA, Nucleic Acids Res. 39 (2011) e142.
[18] K. Karikó, H. Muramatsu, F.A. Welsh, J. Ludwig, H. Kato, S. Akira, D. Weissman, Incorporation of pseudouridine into mRNA yields superior nonimmunogenic vector with increased translational capacity and biological stability, Mol. Ther. 16 (2008) 1833–1840.
[19] M.G. Stanton, K.E. Murphy-Benenato, Messenger RNA as a novel therapeutic approach, in: RNA Therapeutics, Springer, 2017, pp. 237–253.
[20] L. Zangi, K.O. Lui, A. Von Gise, Q. Ma, W. Ebina, L.M. Ptaszek, D. Später, H. Xu, M. Tabebordbar, R. Gorbatov, Modified mRNA directs the fate of heart progenitor cells and induces vascular regeneration after myocardial infarction, Nat. Biotechnol. 31 (2013) 898–907.
[21] A. Magadum, N. Singh, A.A. Kurian, M.T.K. Sharkar, E. Chepurko, L. Zangi, Ablation of a single N-glycosylation site in human FSTL 1 induces cardiomyocyte proliferation and cardiac regeneration, Mol. Ther. Nucleic Acids 13 (2018) 133–143.
[22] F. van den Akker, D.A. Feyen, P. van den Hoogen, L.W. van Laake, E.C. van Eeuwijk, I. Hoefer, G. Pasterkamp, S.A. Chamuleau, P.F. Grundeman, P. A. Doevendans, J.P. Sluijter, Intramyocardial stem cell injection: go(ne) with the flow, Eur. Heart J. 38 (2017) 184–186.
[23] V.J. Caride, B.L. Zaret, Liposome accumulation in regions of experimental myocardial infarction, Science 198 (1977) 735–738.
[24] I.E. Allijn, B.M. Czarny, X. Wang, S.Y. Chong, M. Weiler, A.E. Da Silva, J. M. Metselaar, C.S.P. Lam, G. Pastorin, D.P. de Kleijn, Liposome encapsulated berberine treatment attenuates cardiac dysfunction after myocardial infarction, J. Control. Release 247 (2017) 127–133.
[25] M. Jayaraman, S.M. Ansell, B.L. Mui, Y.K. Tam, J. Chen, X. Du, D. Butler, L. Eltepu, S. Matsuda, J.K. Narayanannair, Maximizing the potency of siRNA lipid nanoparticles for hepatic gene silencing in vivo, Angew. Chem. 124 (2012) 8657–8661.

[26] L. Warren, P.D. Manos, T. Ahfeldt, Y.-H. Loh, H. Li, F. Lau, W. Ebina, P.K. Mandal, Z.D. Smith, A. Meissner, Highly efficient reprogramming to pluripotency and directed differentiation of human cells with synthetic modified mRNA, Cell Stem Cell 7 (2010) 618–630.
[27] M.Y. Arteta, T. Kjellman, S. Bartesaghi, S. Wallin, X. Wu, A.J. Kvist, A. Dabkowska, N. Székely, A. Radulescu, J. Bergenholtz, Successful reprogramming of cellular protein production through mRNA delivered by functionalized lipid nanoparticles, Proc. Natl. Acad. Sci. 115 (2018) E3351–E3360.
[28] R. Jain, J.P. Frederick, E.Y. Huang, K.E. Burke, D.M. Mauger, E.A. Andrianova, S. J. Farlow, S. Siddiqui, J. Pimentel, K. Cheung-Ong, MicroRNAs enable mRNA therapeutics to selectively program cancer cells to self-destruct, Nucleic Acid Ther. 28 (2018) 285–296.
[29] R.D. Brown, S.K. Ambler, M.D. Mitchell, C.S. Long, The cardiac fibroblast: therapeutic target in myocardial remodeling and failure, Annu. Rev. Pharmacol. Toxicol. 45 (2005) 657–687.
[30] E. Shantsila, B.J. Wrigley, A.D. Blann, P.S. Gill, G.Y. Lip, A contemporary view on endothelial function in heart failure, Eur. J. Heart Fail. 14 (2012) 873–881.
[31] A. Yndestad, J.K. Damås, E. Øie, T. Ueland, L. Gullestad, P. Aukrust, Role of inflammation in the progression of heart failure, Curr. Cardiol. Rep. 9 (2007) 236–241.
[32] R. Münter, K. Kristensen, D. Pedersbæk, J.B. Larsen, J.B. Simonsen, T.L. Andresen, Dissociation of fluorescently labeled lipids from liposomes in biological environments challenges the interpretation of uptake studies, Nanoscale 10 (2018) 22720–22724.
[33] Y. Liu, Y.-C. Tseng, L. Huang, Biodistribution studies of nanoparticles using fluorescence imaging: a qualitative or quantitative method? Pharm. Res. 29 (2012) 3273–3277.
[34] F. Meng, J. Wang, Q. Ping, Y. Yeo, Quantitative assessment of nanoparticle biodistribution by fluorescence imaging, revisited, ACS Nano 12 (2018) 6458–6468.
[35] N. Pardi, S. Tuyishime, H. Muramatsu, K. Kariko, B.L. Mui, Y.K. Tam, T.D. Madden, M.J. Hope, D. Weissman, Expression kinetics of nucleoside-modified mRNA delivered in lipid nanoparticles to mice by various routes, J. Control. Release 217 (2015) 345–351.
[36] R.F. Kwekkeboom, J.P. Sluijter, B.J. van Middelaar, C.H. Metz, M.A. Brans, O. Kamp, W.J. Paulus, R.J. Musters, Increased local delivery of antagomir therapeutics to the rodent myocardium using ultrasound and microbubbles, J. Control. Release 222 (2016) 18–31.
[37] J.E. Dahlman, K.J. Kauffman, Y. Xing, T.E. Shaw, F.F. Mir, C.C. Dlott, R. Langer, D. G. Anderson, E.T. Wang, Barcoded nanoparticles for high throughput in vivo discovery of targeted therapeutics, Proc. Natl. Acad. Sci. 114 (2017) 2060–2065.
[38] L. Carlsson, J.C. Clarke, C. Yen, F. Gregoire, T. Albery, M. Billger, A.-C. Egnell, L.-M. Gan, K. Jennbacken, E. Johansson, Biocompatible, purified VEGF-A mRNA improves cardiac function after intracardiac injection 1 week post-myocardial infarction in swine, Mol. Ther. Meth. Clin. Dev. 9 (2018) 330–346.
[39] J. Chen, Q. Ma, J.S. King, Y. Sun, B. Xu, X. Zhang, S. Zohrabian, H. Guo, W. Cai, G. Li, aYAP modRNA reduces cardiac inflammation and hypertrophy in a murine ischemia-reperfusion model, Life Sci. Alliance 3 (2020).
[40] Y. Hadas, A.S. Vincek, E. Youssef, M.M. Żak, E. Chepurko, N. Sultana, M.T. K. Sharkar, N. Guo, R. Komargodski, A.A. Kurian, Altering sphingolipid metabolism attenuates cell death and inflammatory response after myocardial infarction, Circulation 141 (2020) 916–930.
[41] C.-L. Huang, A.-L. Leblond, E.C. Turner, A.H. Kumar, K. Martin, D. Whelan, D. M. O'Sullivan, N.M. Caplice, Synthetic chemically modified mrna-based delivery of cytoprotective factor promotes early cardiomyocyte survival post-acute myocardial infarction, Mol. Pharm. 12 (2015) 991–996.
[42] A. Magadum, N. Singh, A.A. Kurian, I. Munir, T. Mehmood, K. Brown, M.T. K. Sharkar, E. Chepurko, Y. Sassi, J.G. Oh, Pkm2 regulates cardiomyocyte cell cycle and promotes cardiac regeneration, Circulation 141 (2020) 1249–1265.
[43] N. Sultana, Y. Hadas, M.T.K. Sharkar, K. Kaur, A. Magadum, A.A. Kurian, N. Hossain, B. Alburquerque, S. Ahmed, E. Chepurko, Optimization of 5′ untranslated region of modified mRNA for use in cardiac or hepatic ischemic injury, Mol. Ther. Meth. Clin. Dev. 17 (2020) 622–633.
[44] N. Sultana, A. Magadum, Y. Hadas, J. Kondrat, N. Singh, E. Youssef, D. Calderon, E. Chepurko, N. Dubois, R.J. Hajjar, Optimizing cardiac delivery of modified mRNA, Mol. Ther. 25 (2017) 1306–1315.
[45] I.C. Turnbull, A.A. Eltoukhy, K.M. Fish, M. Nonnenmacher, K. Ishikawa, J. Chen, R. J. Hajjar, D.G. Anderson, K.D. Costa, Myocardial delivery of lipidoid nanoparticle carrying modRNA induces rapid and transient expression, Mol. Ther. 24 (2016) 66–75.
[46] Z. Lei, J. Fang, J.C. Deddens, C.H.G. Metz, E.C.M. van Eeuwijk, H. El Azzouzi, P. A. Doevendans, J.P.G. Sluijter, Loss of miR-132/212 has no Long-term beneficial effect on cardiac function after permanent coronary occlusion in mice, Front. Physiol. 11 (2020) 590.
[47] R.A. de Boer, G. De Keulenaer, J. Bauersachs, D. Brutsaert, J.G. Cleland, J. Diez, X. J. Du, P. Ford, F.R. Heinzel, K.E. Lipson, Towards better definition, quantification and treatment of fibrosis in heart failure. A scientific roadmap by the Committee of Translational Research of the heart failure association (HFA) of the European Society of Cardiology, Eur. J. Heart Fail. 21 (2019) 272–285.
[48] H. Ma, L. Wang, C. Yin, J. Liu, L. Qian, In vivo cardiac reprogramming using an optimal single polycistronic construct, Cardiovasc. Res. 108 (2015) 217–219.
[49] L. Qian, Y. Huang, C.I. Spencer, A. Foley, V. Vedantham, L. Liu, S.J. Conway, J. D. Fu, D. Srivastava, In vivo reprogramming of murine cardiac fibroblasts into induced cardiomyocytes, Nature 485 (2012) 593–598.
[50] A. Magadum, K. Kaur, L. Zangi, mRNA-based protein replacement therapy for the heart, Mol. Ther. 27 (2019) 785–793.